Nucleophilic Substitution by a Hydroxide Ion at a Vinylic Carbon: Ab Initio and Density Functional Theory Studies on Methoxyethene, 3-Methoxypropenal, 2,3-Dihydro-4*H*-pyran-4-one, and 4*H*-Pyran-4-one

Juraj Kóňa,*,† Pavol Zahradník,‡ and Walter M. F. Fabian*,†

Institut für Chemie, Karl-Franzens Universität Graz, Heinrichstr. 28, A-8010 Graz, Austria, and Department of Organic Chemistry, Comenius University Bratislava, Mlynska dolina CH-2, SK-842 15 Bratislava, Slovak Republic

walter.fabian@uni-graz.at

Received August 10, 2000

Nucleophilic substitutions by a hydroxide ion at vinylic carbons of methoxyethene (system A), 3-methoxypropenal (system B), 2,3-dihydro-4*H*-pyran-4-one (system C), and 4*H*-pyran-4-one (system D) were calculated by Becke's three-parameter hybrid density functional-HF method with the Lee−Yang−Parr correlation functional (B3LYP//B3LYP) and the second-order Møller−Plesset theory (MP2//B3LYP) using the 6-31+G(d) and AUG-cc-pVTZ basis sets. In addition, bulk solvent effects (aqueous solution) were estimated by the polarized continuum (overlapping spheres) model (PCM-B3LYP//B3LYP) and the polarizable conductor PCM model (CosmoPCM-B3LYP//B3LYP). The mechanisms as well as the influence of resonance, cyclic strain, aromatic, and polar effects on the reactivity of the calculated systems were determined. In the gas phase the rate-determining step of nucleophilic vinylic substitutions by a hydroxide ion may be either addition of hydroxide ion at the vinylic carbon (systems A and B) or elimination of the leaving group (systems C and D). In aqueous solution, for all four systems investigated, addition of hydroxide ion at the vinylic carbon is rate determining.

Introduction

Six-membered oxygen heterocycles constitute a group of compounds, which occur widely throughout the plant kingdom.[1] The ketones derived from pyrans known as pyranones and their benzologues play different roles in plant physiology and exhibit a diverse spectrum of biological functions.[2] They are interesting as pharmacological agents since they stimulate or inhibit a wide variety of enzyme systems[3] and have potential as antibacterial, anticancer, and antiallergy agents.[4]

Many experimental and theoretical works were dedicated to the question of their aromatic properties.[5] The electronic structure of the heterocyclic ring of 4*H*-pyran-4-one fulfills the conditions for aromatic Hückel systems.[6] Despite this, several properties of the γ-pyrone ring can also be satisfactorily explained in terms of an aliphatic dienone system. From this point of view, the structural configuration C═C−C═O of 4*H*-pyran-4-ones (γ-pyrones) and their benzologues (chromones and flavones) is similar to α,β-unsaturated carbonyl compounds. However, some of their properties are unexpected on this basis. First, the carbonyl group is devoid of normal ketonic properties such as hydrazone or oxime formation. The system does not react normally with oxygen and nitrogen nucleophiles. Instead, cleavage of the heterocyclic ring occurs. In general, depending on the pH conditions, γ-pyrones and their benzologues are susceptible to nucleophilic attack at the positions C2 and C4 of the heterocyclic ring.[5b,7] Under basic conditions the attack takes place at

* To whom correspondence should be addressed. Fax: +43 316 3809840

† Karl-Franzens Universität Graz.

‡ Comenius University.

(1) Staunton, J. In *Comprehensive Organic Chemistry, The Synthesis and Reactions of Organic Compounds*; Barton, D., Ollis, W. D., Eds.; Pergamon Press: Oxford, 1979; Vol. 4, pp 679, 688.

(2) (a) Havsteen, B. *Biochem. Pharmacol.* **1983**, *32*, 1141. (b) Koes, R. E.; Quattrocchio; F.; Mol, J. N. M. *BioEssays* **1994**, *16*, 123.

(3) (a) Ferriola, P. C.; Cody, V.; Middleton, E., Jr. *Biochem. Pharmacol.* **1989**, *38*, 1617. (b) Brinkworth, R. I.; Stoermer, M. J.; Fairlie, D. P. *Biochem. Biophys. Res. Commun.* **1992**, *188*, 631. (c) Elliott, A. J.; Scheiber, S. A.; Thomas, C.; Pardini, R. S. *Biochem. Pharmacol.* **1992**, *44*, 1603. (d) Laughton, M. J.; Evans, P. J.; Moroney, M. A.; Hoult, J. R. S.; Halliwell, B. *Biochem. Pharmacol.* **1991**, *42*, 1673. (e) Middleton, E., Jr.; Drzewiecki, G. *Biochem. Pharmacol.* **1982**, *31*, 1449.

(4) (a) Ellis, G. P. In *The Chemistry of Heterocyclic Compounds, Chromenes, Chromanones and Chromones*; Weissberger, A., Taylor, E. C., Eds.; Wiley: New York, 1977; Vol. 31, pp 912, 985, 1063. (b) Cox, J. S. G.; Beach, J. E.; Blair, A. M. N.; Clarke, A. J.; King, J.; Lee, T. B.; Loveday, D. E. E.; Moss, G. F.; Orr, T. S. C.; Ritchie, J. T.; Sherd, P. *Adv. Drug Res.* **1970**, *5*, 115. (c) Ellis, G. P.; Shaw, D. *J. Chem. Soc., Perkin Trans. 1* **1972**, 776. (d) Ellis, G. P.; Shaw, D. *J. Med. Chem.* **1972**, *15*, 865. (e) Nohara, A.; Kuriki, H.; Saijo, T.; Ukawa, K.; Murata, T.; Kanno, M.; Sanno, Y. *J. Med. Chem.* **1975**, *18*, 34. (f) Nohara, A.; Kuriki, H.; Saijo, T.; Sugihara, H.; Kanno, M.; Sanno, Y. *J. Med. Chem.* **1977**, *20*, 141. (g) Ellis, G. P.; Becket, G. J. P.; Shaw, D.; Wilson, H. K.; Vardey, C. J.; Skidmore, I. F. *J. Med. Chem.* **1978**, *21*, 1120. (h) Nakai, H.; Konno, M.; Kossuge, S.; Sakuyama, S.; Toda, M.; Arai, Y.; Obata, T.; Katsube, N.; Miyamoto, T.; Okegawa, T.; Kawasaki, A. *J. Med. Chem.* **1988**, *31*, 84.

(5) (a) Hepworth, J. D.; Gabbutt, C. D.; Heron, B. M. In *Comprehensive Heterocyclic Chemistry II, A review of the Literature 1982−1995*; Katritzky, R., Rees C. W., Scriven, E. F., Eds.; Pergamon: Oxford, 1996; Vol. 5, p 341. (b) Brogden, P. J.; Gabbutt, C. D.; Hepworth, J. D. In *Comprehensive Heterocyclic Chemistry, The Structure, Reactions, Synthesis and Uses of Heterocyclic Compounds*; Katritzky, R., Rees, C. W., Eds.; Pergamon Press: Oxford, 1984; Vol. 3, pp 573, 698.

(6) March, J. In *Advanced Organic Chemistry, Reactions, Mechanisms, and Structure*; Wiley: New York, 1992; pp 51, 335, 741.

(7) (a) Morin, C.; Beugelmans, R. *Tetrahedron* **1977**, *33*, 3183. (b) Szabó, V.; Borda J.; Losonczi, L. *Acta Chim. Acad. Sci. Hung.* **1978**, *97*, 69. (c) Szabó, V.; Borda, J.; Végh, V. *Acta Chim. Acad. Sci. Hung.* **1978**, *98*, 457. (d) Beugelmans, R.; Morin, C. *J. Org. Chem.* **1977**, *42*, 1356.

10.1021/jo001222i CCC: $20.00
Published on Web 06/22/2001

C2 followed by fission of the heterocyclic ring. This process is analogous to nucleophilic addition at the β-carbon of the α,β-unsaturated carbonyl compounds or nucleophilic vinylic substitution (NVS). The mechanism of these nucleophilic ring-opening reactions was studied experimentally[8] as well as by quantum-chemical calculations.[9] They can be classified as NVS[8a−c,9] according to an addition−elimination mechanism.[6,10]

Most of the theoretical works were done for the reactions of acrolein with various nucleophiles,[11] but to the best of our knowledge quantum-chemical calculations on the mechanism of NVS at the activated double bond with RO^- as the leaving group have not been published yet. To better understand the specific nature of the γ-pyrone ring, mainly the effects of its cyclic and aromatic properties on the reactivity of C2, we perform ab initio and density functional theory calculations on 4*H*-pyran-4-one with hydroxide ion in the gas phase and aqueous solution (Scheme 1, system D). In addition, calculations on the reactions of methoxyethene (system A), 3-methoxypropenal (system B) and 2,3-dihydro-4*H*-pyran-4-one (system C) with hydroxide ion are presented (Scheme 1). Systems A, B, and C are only theoretical models and comparison of their structure−reactivity data with those of 4*H*-pyran-4-one can reveal a complex interplay of electronic, resonance, and steric effects in the γ-pyrone ring. The simulated reaction substrates were gradually constructed from methoxyethene to 4*H*-pyran-4-one by adding the following structural fragments: the activating carbonyl group (systems B, C, and D), $-CH_2-CH_2-$ fragment (system C, a cyclic system with the activating group), and $-CH=CH-$ fragment (system D, a cyclic aromatic system with the activating group). System A does not contain any of the above-mentioned structural features and presents a basic model for our computational simulations of NVS. The reactions were simulated as bimolecular according to the well-established addition−elimination mechanism.[10b−e]

Scheme 1

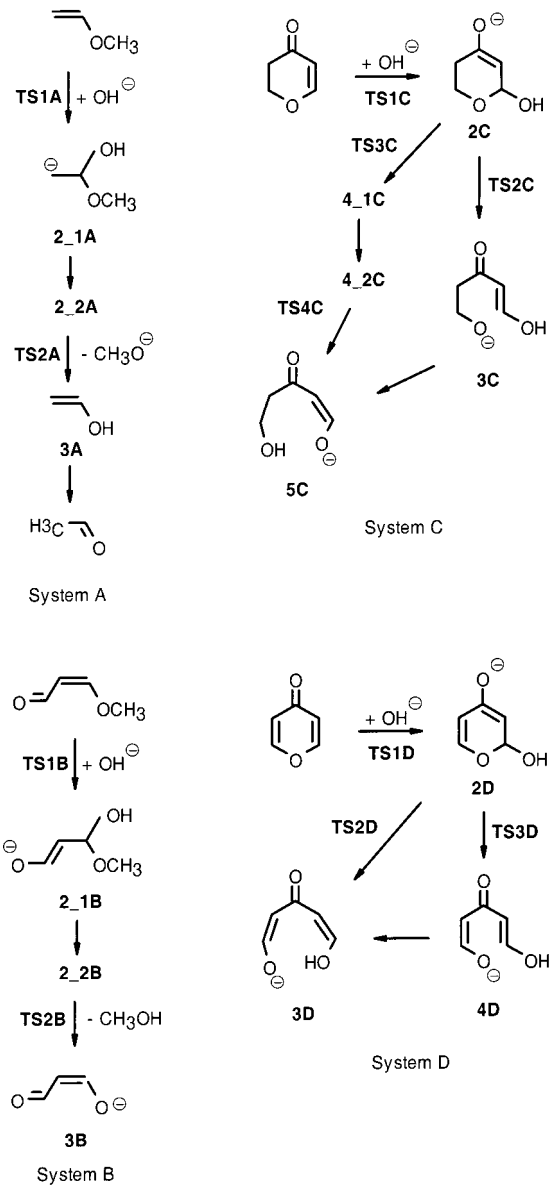

Computational Methods

All calculations were performed by the Gaussian 98 program package.[12] Geometries were completely optimized with the aid of Becke's three-parameter hybrid density functional-HF method with the Lee−Yang−Parr correlation functional[13] (B3LYP//B3LYP) using the 6-31+G(d) basis set.[14] In addition, correlation energy was also evaluated using the second-order Møller−Plesset theory[15] by single point calculations at the B3LYP geometries (MP2//B3LYP) using the 6-31+G(d) basis set.[14] To check basis set effects, Dunning's correlation consistent triple-ζ basis set[16] augmented by diffuse functions (AUG-cc-pVTZ) was tested employing the B3LYP//B3LYP and PCM-B3LYP//B3LYP levels of theory. All stationary points were characterized as minima or transition states by vibrational

(8) (a) Davidson, D. N.; English, R. B.; Kaye, P. T. *J. Chem. Soc., Perkin Trans. 2* **1991**, 1509. (*b*) Szabó, V.; Zsuga, M. *Acta Chim. Acad. Sci. Hung.* **1975**, *85*, 179, 191; **1978**, *97*, 451. (*c*) Zsuga, M.; Szabó, V.; Kóródi, F.; Kiss, A. *Acta Chim. Acad. Sci. Hung.* **1979**, *101*, 73. (d) Beak, P.; Carls, G. A. *J. Org. Chem.* **1964**, *29*, 2678. (e) Mayo, D. W.; Sapienza, P. J.; Lord, R. C.; Phillips, W. D. *J. Org. Chem.* **1964**, *29*, 2682 (f) Ichimoto, I.; Kitaoka, Y.; Tatsumi, C. *Tetrahedron* **1966**, *22*, 841. (g) Zagorevskii, V. A.; Orlova, E. K.; Tsvetkova, I. D. *Chem. Heterocycl. Compd. (Engl. Transl.)* **1972**, *8*, 416.

(9) Kóňa, J.; Fabian, W. M. F.; Zahradník, P. *J. Chem. Soc., Perkin Trans. 2* **2001**, 422.

(10) (a) Bernasconi, C. F. *Tetrahedron* **1989**, *45*, 4017. (b) Bernasconi, C. F.; Schuck, D. F.; Ketner, R. J.; Weiss, M.; Rappoport, Z. *J. Am. Chem. Soc.* **1994**, *116*, 11764. (c) Bernasconi, C. F.; Ketner, R. J.; Chen, X.; Rappoport, Z. *J. Am. Chem. Soc.* **1998**, *120*, 7461. (d) Bernasconi, C. F.; Fassberg, J.; Killion, R. B., Jr.; Schuck, D. F.; Rappoport, Z. *J. Am. Chem. Soc.* **1991**, *113*, 4937. (e) Bernasconi, C. F.; Ketner, R. J.; Chen, X.; Rappoport, Z. *Can. J. Chem.* **1999**, *77*, 584.

(11) (a) Thomas IV, B. E.; Kollman, P. A. *J. Org. Chem.* **1995**, *60*, 8375. (b) Bayly, C. I.; Grein, F. *Can. J. Chem.* **1989**, *67*, 2173. (c) Pardo, L.; Osman, R. L.; Weinstein, H.; Rabinowitz, J. R. *J. Am. Chem. Soc.* **1993**, *115*, 8263. (d) Wong, S. S.; Paddon-Row, M. N.; Li, Y.; Houk, K. N. *J. Am. Chem. Soc.* **1990**, *112*, 8679.

(12) Frisch, M. J.; Trucks, G. W.; Schlegel, H. B.; Scuseria, G. E.; Robb, M. A.; Cheeseman, J. R.; Zakrzewski, V. G.; Montgomery, J. A.; Stratmann, R. E.; Burant, J. C.; Dapprich, S.; Millam, J. M.; Daniels, A. D.; Kudin, K. N.; Strain, M. C.; Farkas, O.; Tomasi, J.; Barone, V.; Cossi, M.; Cammi, R.; Mennucci, B.; Pomelli, C.; Adamo, C.; Clifford, S.; Ochterski, J.; Petersson, G. A.; Ayala, P. Y.; Cui, Q.; Morokuma, K.; Malick, D. K.; Rabuck, A. D.; Raghavachari, K.; Foresman, J. B.; Cioslowski, J.; Ortiz, J. V.; Stefanov, B. B.; Liu, G.; Liashenko, A.; Piskorz, P.; Komaromi, I.; Gomperts, R.; Martin, R. L.; Fox, D. J.; Keith, T.; Al-Laham, M. A.; Peng, C. Y.; Nanayakkara, A.; Gonzalez, C.; Challacombe, M.; Gill, P. M. W.; Johnson, B. G.; Chen, W.; Wong, M. W.; Andres, J. L.; Head-Gordon, M.; Replogle, E. S.; Pople, J. A. *Gaussian 98*, Revision A.7; Gaussian, Inc.: Pittsburgh, PA, 1998.

(13) (a) Becke, A. D. *J. Chem. Phys.* **1993**, *98*, 5648. (b) Lee, C.; Yang, W.; Parr, R. G. *Phys. Rev. B* **1988**, *37*, 785. (c) Miehlich, B.; Savin, A.; Stoll, H.; Preuss, H. *Chem. Phys. Lett.* **1989**, *157*, 200.

(14) (a) Hehre, W. J.; Ditchfield, R.; Pople, J. A. *J. Chem. Phys.* **1972**, *56*, 2257. (b) Hariharan, P. C.; Pople, J. A. *Mol. Phys.* **1974**, *27*, 209. (c) Hariharan, P. C.; Pople, J. A. *Theor. Chim. Acta* **1973**, *28*, 213.

(15) (a) Møller, C.; Plesset, M. S. *Phys. Rev.* **1934**, *46*, 618. (b) Head-Gordon, M.; Pople, J. A.; Frisch, M. J. *Chem. Phys. Lett.* **1988**, *153*, 503. (*c*) Frisch, M. J.; Head-Gordon, M.; Pople, J. A. *Chem. Phys. Lett.* **1990**, *166*, 275, 281.

Table 1. Calculated Relative Energies (E_{rel})[a] Including ZPE Corrections of the Various Minima and Transition States for the Reactions of Methoxyethene (system A) and 3-methoxypropenal (system B) with Hydroxide Ion in the Gas Phase and Aqueous Solution Depicted in Scheme 1 (in kJ mol^{-1})

	E_{rel}[b]	E_{rel}[c]	E_{rel}[d]	E_{rel}[e]	E_{rel}[f]	E_{rel}[g]
1A	−49	−46	−48	33	49	174
TS1A	−2	5	0	137	149	201
2_1A	−16	−6	−19	169	174	200
2_2A	−23	−11	−26	158	170	198
TS2A	−13	−6	−5	146	173	187
3A	−68	−64	−51	58	83	89
1B	−139	−128	−135	24	44	
TS1B	−114	−103	−106	56	71	142
2_1B	−176	−159	−182	23	36	
2_2B	−163	−146	−170	38	49	
TS2B	−147	−131	−137	76	100	139
3B	−308	−292	−296	−61	−44	

[a] Energies are given relative to the separated reactants. [b] B3LYP/6-31+G(d)//B3LYP/6-31+G(d). [c] B3LYP/AUG-cc-pVTZ//B3LYP/6-31+G(d). [d] MP2/6-31+G(d)//B3LYP/6-31+G(d). [e] PCM-B3LYP/6-31+G(d)//B3LYP/6-31+G(d). [f] CosmoPCM-B3LYP/6-31+G(d)//B3LYP/6-31+G(d). [g] PCM-B3LYP/AUG-cc-pVTZ//B3LYP/6-31+G(d).

Table 2. Calculated Activation Energies ($\Delta E^{\ddagger}$) for the Reactions of Methoxyethene (system A) and 3-methoxypropenal (system B) with Hydroxide Ion in the Gas Phase and Aqueous Solution Depicted in Scheme 1 (in kJ mol^{-1})

	$\Delta E^{\ddagger a}$	$\Delta E^{\ddagger b}$	$\Delta E^{\ddagger c}$	$\Delta E^{\ddagger d}$	$\Delta E^{\ddagger e}$	$\Delta E^{\ddagger f}$
$\Delta E_{1A}^{\ddagger}$ (**1A** → **TS1A**)[g]	47	51	47	137	149	201
$\Delta E_{2A}^{\ddagger}$ (**2_2A** → **TS2A**)	10	5	22	−12	2	−11
$\Delta E_{1B}^{\ddagger}$ (**1B** → **TS1B**)[g]	24	24	29	56	71	
$\Delta E_{2B}^{\ddagger}$ (**2_2B** → **TS2B**)	16	15	32	38	52	

[a] B3LYP/6-31+G(d)//B3LYP/6-31+G(d). [b] B3LYP/AUG-cc-pVTZ//B3LYP/6-31+G(d). [c] MP2/6-31+G(d)//B3LYP/6-31+G(d). [d] PCM-B3LYP/6-31+G(d)//B3LYP/6-31+G(d). [e] CosmoPCM-B3LYP/6-31+G(d)//B3LYP/6-31+G(d). [f] PCM-B3LYP/AUG-cc-pVTZ//B3LYP/6-31+G(d). [g] $\Delta E_{1A}^{\ddagger}$ (reactants → **TS1A**) and $\Delta E_{1B}^{\ddagger}$ (reactants → **TS1B**) for the PCM-B3LYP//B3LYP and CosmoPCM-B3LYP//B3LYP models.

frequency calculations. In addition, for transition states, intrinsic reaction coordinate (IRC) calculations at the B3LYP//B3LYP level of theory were performed. Thermodynamic quantities were calculated at 298 K and 101.325 kPa using standard rigid-rotor harmonic oscillator partition function expressions. Zero-point energies (ZPE) are unscaled.

Bulk solvent effects (aqueous solution, $\epsilon = 78.39$) were estimated by single-point calculations using the polarized continuum (overlapping spheres) model[17] (PCM-B3LYP//B3LYP) and polarizable conductor PCM model[18] (CosmoPCM-B3LYP//B3LYP) using the 6-31+G(d)[14] and AUG-cc-pVTZ[16] basis sets.

Results

Relative energies (E_{rel}) including ZPE contributions for the gas phase and aqueous solution are summarized in Tables 1 (systems A and B), 3 (system C) and 4 (system D). Activation energies ($\Delta E^{\ddagger}$) for the individual reaction steps are presented in Tables 2 (systems A and B) and 5 (systems C and D). Structural features for all transition

Table 3. Calculated Relative Energies (E_{Rel})[a] Including ZPE Corrections of the Various Minima and Transition States for the Reaction of 2,3-dihydro-4*H*-pyran-4-one (system C) with Hydroxide Ion in the Gas Phase and Aqueous Solution Depicted in Scheme 1 (in kJ mol^{-1})

	E_{rel}[b]	E_{rel}[c]	E_{rel}[d]	E_{rel}[e]	E_{rel}[f]
1C	−86	−80	−82	47	62
TS1C	−75	−68	−75	62	74
				(165)[g]	
2C	−173	−156	−180	35	47
TS2C	−91	−79	−76	82	103
				(160)[g]	
3C	−110	−99	−94	55	76
TS3C	−149	−133	−153	61	73
4_1C	−168	−151	−174	36	48
4_2C	−148	−133	−154	44	55
TS4C	−90	−318	−86	125	145
				(180)[g]	
5C	−268	−68	−262	−26	−10

[a] Energies are given relative to the separated reactants. [b] B3LYP/6-31+G(d)//B3LYP/6-31+G(d). [c] B3LYP/AUG-cc-pVTZ//B3LYP/6-31+G(d). [d] MP2/6-31+G(d)//B3LYP/6-31+G(d). [e] PCM-B3LYP/6-31+G(d)//B3LYP/6-31+G(d). [f] CosmoPCM-B3LYP/6-31+G(d)//B3LYP/6-31+G(d). [g] PCM-B3LYP/AUG-cc-pVTZ//B3LYP/6-31+G(d).

Table 4. Calculated Relative Energies (E_{rel})[a] Including ZPE Corrections of the Various Minima and Transition States for the Reaction of 4*H*-pyran-4-one (system D) with Hydroxide Ion in the Gas Phase and Aqueous Solution Depicted in Scheme 1 (in kJ mol^{-1})

	E_{rel}[b]	E_{rel}[c]	E_{rel}[d]	E_{rel}[e]	E_{rel}[f]
1D	−117	−110	−112	72	88
TS1D	−87	−80	−80	96	114
2D	−159	−142	−176	24	44
TS2D	−116	−100	−117	71	88
3D	−260	−245	−243	−29	−5
TS3D	−123	−106	−121	54	74
4D	−213	−199	−197	−9	12

[a] Energies are given relative to the separated reactants. [b] B3LYP/6-31+G(d)//B3LYP/6-31+G(d). [c] B3LYP/AUG-cc-pVTZ//B3LYP/6-31+G(d). [d] MP2/6-31+G(d)//B3LYP/6-31+G(d). [e] PCM-B3LYP/6-31+G(d)//B3LYP/6-31+G(d). [f] CosmoPCM-B3LYP/6-31+G(d)//B3LYP/6-31+G(d).

Table 5. Calculated Activation Energies ($\Delta E^{\ddagger}$) for the Reactions of 2,3-dihydro-4*H*-pyran-4-one (system C) and 4*H*-pyran-4-one (system D) with Hydroxide Ion in the Gas Phase and Aqueous Solution Depicted in Scheme 1 (in kJ mol^{-1})

	$\Delta E^{\ddagger a}$	$\Delta E^{\ddagger b}$	$\Delta E^{\ddagger c}$	$\Delta E^{\ddagger d}$	$\Delta E^{\ddagger e}$
$\Delta E_{1C}^{\ddagger}$ (**1C** → **TS1C**)[f]	11	12	7	62	74
$\Delta E_{2C}^{\ddagger}$ (**2C** → **TS2C**)	82	77	104	47	56
$\Delta E_{3C}^{\ddagger}$ (**2C** → **TS3C**)	24	23	27	26	27
$\Delta E_{4C}^{\ddagger}$ (**4_2C** → **TS4C**)	59	60	68	81	90
$\Delta E_{1D}^{\ddagger}$ (**1D** → **TS1D**)[f]	30	30	32	96	114
	(25)[g]				
$\Delta E_{2D}^{\ddagger}$ (**2D** –**TS2D**)	43	43	59	46	44
	(64)[g]				
$\Delta E_{3D}^{\ddagger}$ (**2D** –**TS3D**)	37	36	55	29	30
	(51)[g]				

[a] B3LYP/6-31+G(d)//B3LYP/6-31+G(d). [b] B3LYP/AUG-cc-pVTZ//B3LYP/6-31+G(d). [c] MP2/6-31+G(d)//B3LYP/6-31+G(d). [d] PCM-B3LYP/6-31+G(d)//B3LYP/6-31+G(d). [e] CosmoPCM-B3LYP/6-31+G(d)//B3LYP/6-31+G(d). [f] $\Delta E_{1C}^{\ddagger}$ (**reactants** → **TS1C**) and $\Delta E_{1D}^{\ddagger}$ (**reactants** → **TS1D**) for the PCM-B3LYP//B3LYP and CosmoPCM-B3LYP//B3LYP models. [g] Calculated activation energies for the reaction between 4*H*-1-benzopyran-4-one and hydroxide ion at the B3LYP/6-31+G(d)//B3LYP/6-31+G(d) level of theory.[9]

(16) (a) Woon, D. E.; Dunning, T. H., Jr. *J. Chem. Phys.* **1993**, *98*, 1358. (b) Kendall, R. A.; Dunning, T. H., Jr.; Harrison, R. J. *J. Chem. Phys.* **1992**, *96*, 6796. (c) Dunning, T. H., Jr. *J. Chem. Phys.* **1989**, *90*, 1007. (d) Peterson, K. A.; Woon, D. E.; Dunning, T. H., Jr. *J. Chem. Phys.* **1994**, *100*, 7410. (e) Davidson, E. R. *Chem. Phys. Lett.* **1996**, *260*, 514.

(17) (a) Miertuš, S.; Scrocco, E.; Tomasi, J. *Chem. Phys.* **1981**, *55*, 117. (b) Miertuš, S.; Tomasi, J. *Chem. Phys.* **1982**, *65*, 239. (c) Cossi, M.; Barone, V.; Cammi, R.; Tomasi, J. *Chem. Phys. Lett.* **1996**, *255*, 327.

(18) (a) Barone, V.; Cossi, M. *J. Phys. Chem. A* **1998**, *102*, 1995. (b) Klamt, A.; Schüürmann, G. *J. Chem. Soc., Perkin Trans. 2* **1993**, 799. (c) Klamt, A. *J. Phys. Chem.* **1995**, *99*, 2224; **1996**, *100*, 3349.

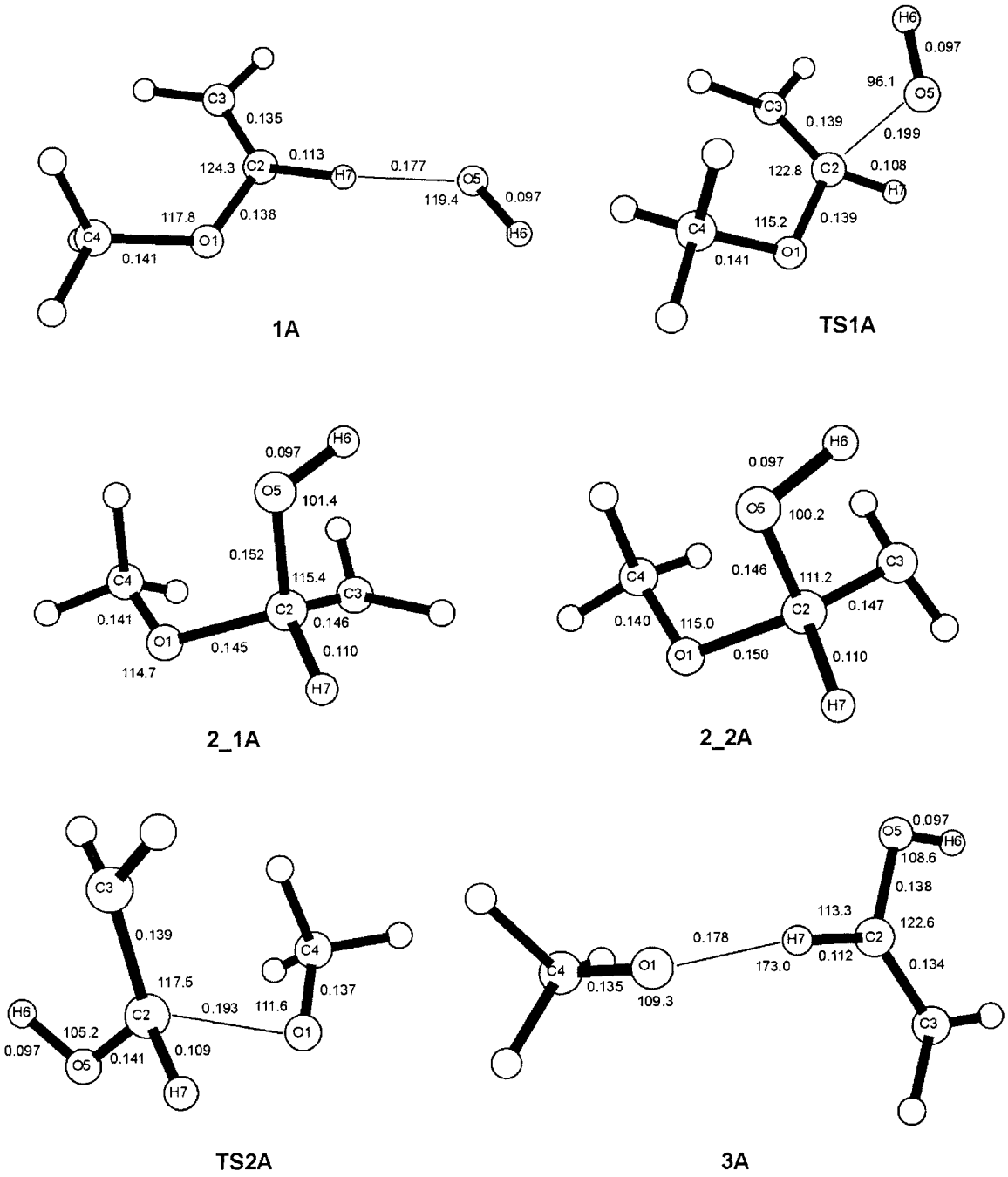

Figure 1. B3LYP calculated structures of the various minima and transition states for nucleophilic vinylic substitution by a hydroxide ion of methoxyethene. Distances are given in nm and bond angles in degrees.

states and minima are shown in Figures 1 (system A), 2 (system B), 3, 4 (system C), and 5 (system D). Relative and total Gibbs free energies, total energies including zero-point energy contributions, and free energies of solvation are provided in the Supporting Information.

First, general features of these reactions will be presented. Then mechanistic and energetic aspects specific for the four reaction systems will be discussed separately. Generally, as one might expect for gas phase reactions involving anionic nucleophiles, all transition states and minima are energetically lower than the separated reactants for all the calculated reactions. Therefore in the gas phase the height of the activation barriers among the individual steps is the most important factor for prediction of the rate-determining step (RDS) of the reaction. Addition of hydroxide ion to vinylic carbons proceeds first by the exothermic formation of ion−dipole complexes **1A**−**D**. These are important for evaluation of activation barriers for the first reaction steps. In contrast, in aqueous solution these complexes are unstable and all transition states as well as tetrahedral intermediates are higher in energy than the corresponding separated reactants. In this case, the RDS will depend on the overall activation energy of the reaction, i.e., the reaction step passing through the transition state, which is the highest in energy overall, will be rate determining.

Common to all four systems is also the formation of a tetrahedral intermediate (Scheme 1). For the acyclic systems A and B these intermediates can adopt more or less freely interconverting conformations. Specifically, according to the IRC calculations, elimination of the

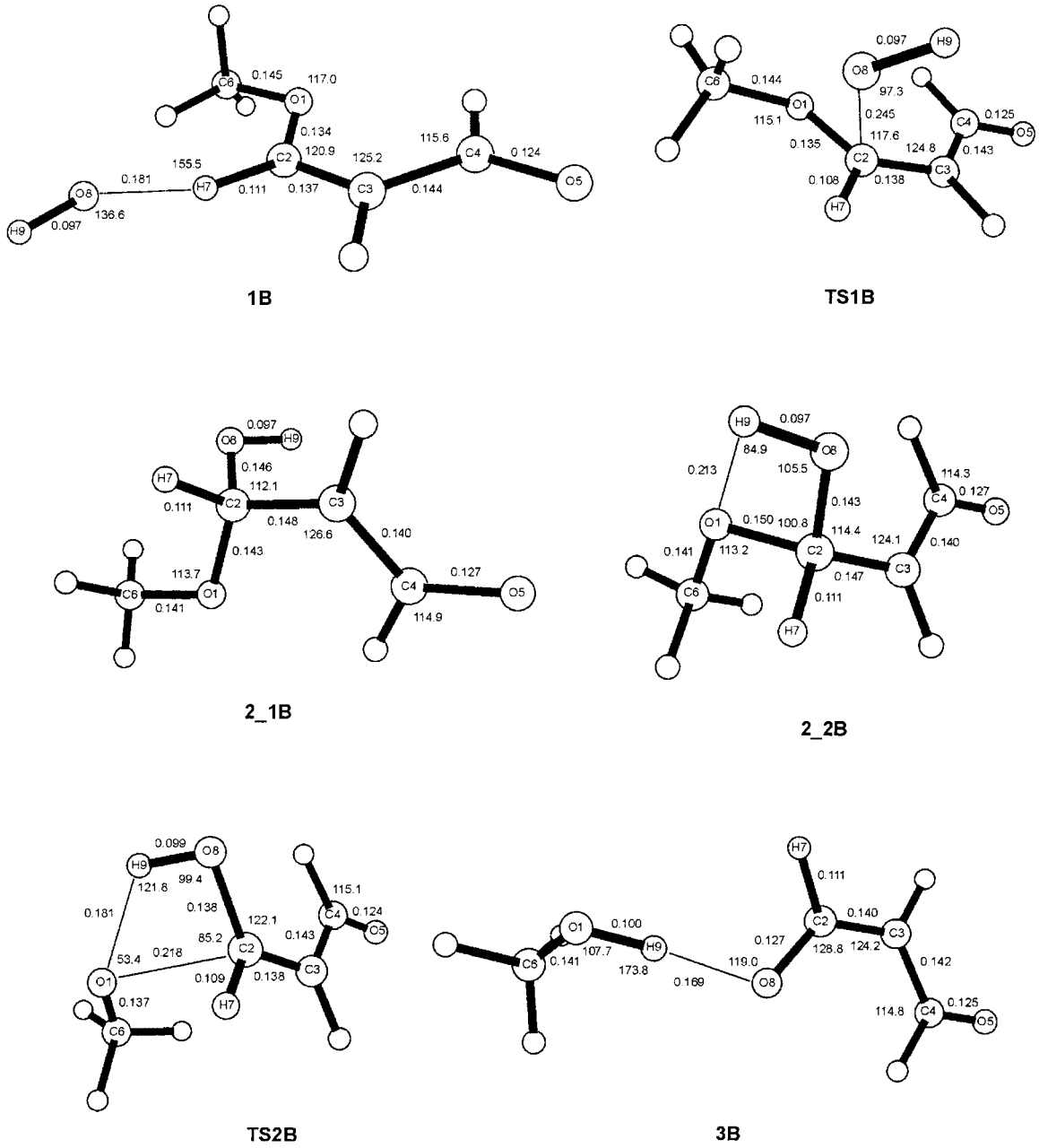

Figure 2. B3LYP calculated structures of the various minima and transition states for nucleophilic vinylic substitution by a hydroxide ion of 3-methoxypropenal. Distances are given in nm and bond angles in degrees.

methoxide (methanol) requires such conformational changes. In the cyclic systems C and D, ring opening (i.e., elimination) may proceed either via inward or outward rotation of the hydroxy group around the C2−C3 bond.

From a methodological point of view, at least for the gas phase, the methods used largely provide consistent results. More problematic appear the solvent calculations using the PCM or CosmoPCM approximation, especially for anionic systems (details, as dependence of solvation free enthalpies on the number of tesserae used in the construction of the cavity as well as escaped charges, are given in Tables S1 and S15−S18 of the Supporting Information). In the range TSNUM = 60−100 calculated activation energies show only little dependence on the number of tesserae. In contrast, geometry optimization with inclusion of the solvent model instead of the usual single point methodology seems to be an important factor as is also the size of the basis set used.

System A. The bimolecular mechanism for NVS of the methoxy group by a hydroxide ion in methoxyethene consists of the following four steps (Scheme 1, Figure 1): addition of hydroxide ion at the vinylic carbon (**1A** → **TS1A** → **2_1A**), conformational interconversion (as evidenced by the IRC calculations) of the tetrahedral intermediate **2_1A** to **2_2A**, elimination of methoxide anion (**2_2A** → **TS2A** → **3A**), and keto−enol tautomerism of the resulting enol to ethanal. The addition and elimination steps were analyzed in more details (the steps **2_1A** → **2_2A** and **3A** → ethanal + $CH_3O^{(-)}$ present reactions, in which low activation barriers are expected and thus should not be significant for the determination of RDS of the reaction).

Structures **2_1A** and **2_2A** present two of the fast interconverting conformers of one intermediate. In contrast to systems B, C and D, no activating group is present in methoxyethene and the maximum negative

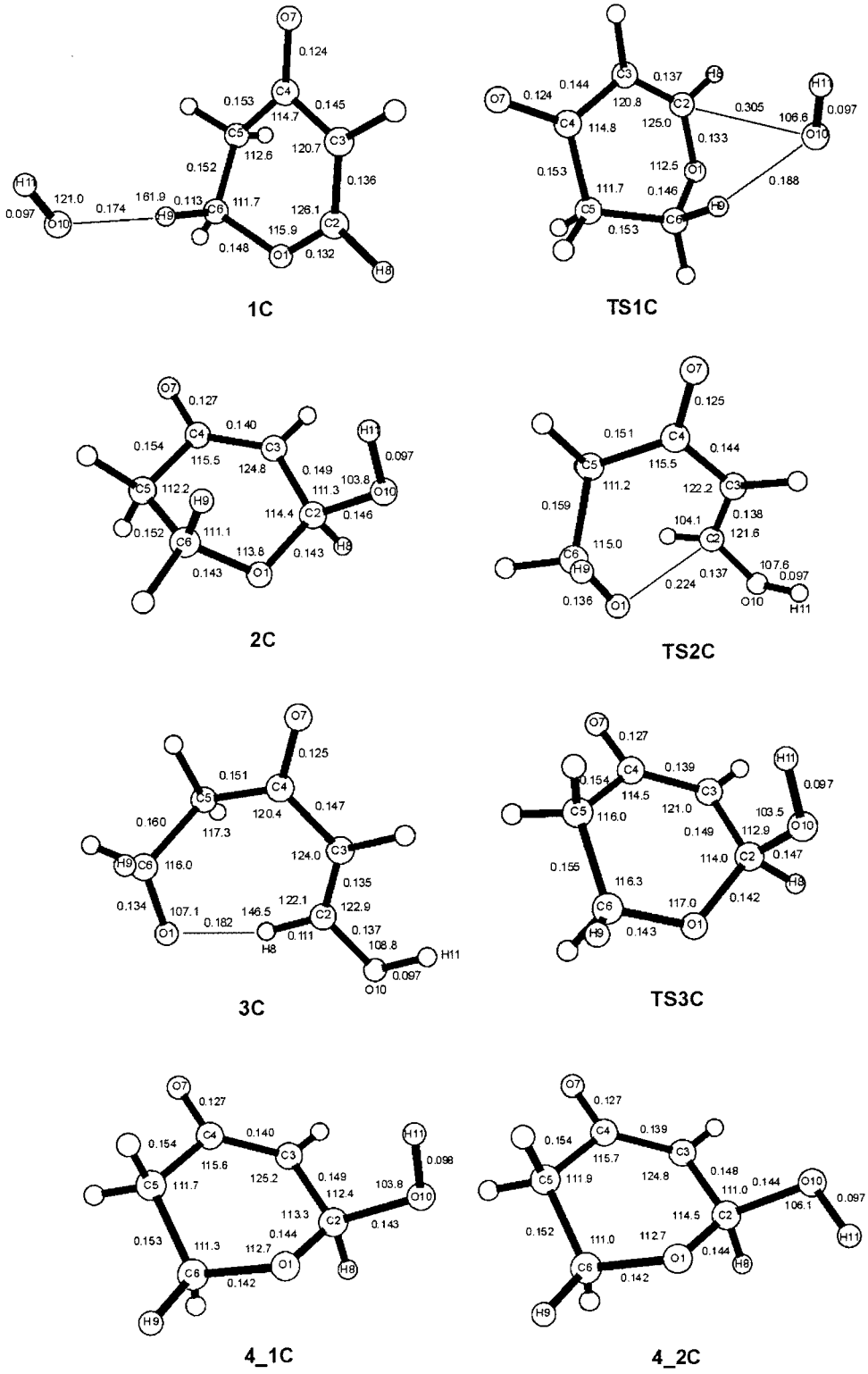

Figure 3. B3LYP calculated structures of the various minima and transition states for nucleophilic vinylic substitution by a hydroxide ion of 2,3-dihydro-4*H*-pyran-4-one. Distances are given in nm and bond angles in degrees.

charge in the tetrahedral intermediates was found to be localized on C3 (−0.54 → −0.90 → −0.79, **1A** → **2_1A** → **2_2A**, B3LYP//B3LYP). Lack of any resonance delocalization seems to be a major reason for the instability of the tetrahedral intermediates in system A (≈ 30 kJ mol^{-1} above the complex **1A**, B3LYP//B3LYP). All methods used predict the highest activation energy for the first step (**1A** → **TS1A** → **2_1A**, $\Delta E_{1A}^{\ddagger} \approx 50$ kJ mol^{-1}, see Table 2). Therefore, addition of hydroxide ion at the vinylic carbon is predicted to be the RDS of the reaction in the gas phase.

Inclusion of bulk solvent effects by the PCM and CosmoPCM models dramatically increases the barrier for the first step (≈140 kJ mol^{-1}). However, none of the two procedures used to describe bulk solvent effects were able to correctly describe the energy profile of this reaction.

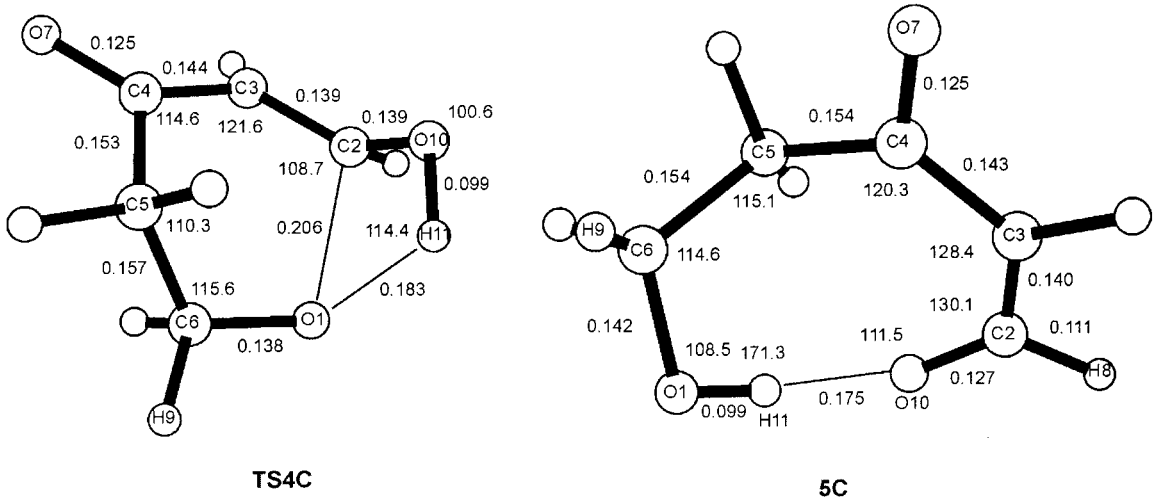

Figure 4. B3LYP calculated structures of transition state **TS4C** and intermediate **5C** for nucleophilic vinylic substitution by a hydroxide ion of 2,3-dihydro-4*H*-pyran-4-one. Distances are given in nm and bond angles in degrees.

Specifically, the tetrahedral intermediates **2__1A** and **2__2A** are calculated to be higher in energy than the respective transition states (see Table 1). As mentioned above, using different numbers of tesserae (TSNUM = 60−100, see Table S1 of the Supporting Information) in the PCM calculations did not significantly alter the results. More important is the use of a larger basis set. For instance, using the AUG-cc-pVTZ basis set in combination with the PCM solvent model [PCM-B3LYP/AUG-cc-pVTZ//B3LYP/6-31+G(d)] predicts the highest energy for **TS1A**, although **TS2A** is still lower in energy than either **2__1A** and **2__2A**. The energy differences are, however, very small (<4 kJ mol^{-1}). Preliminary PCM-B3LYP//PCM-B3LYP calculations,[19] i.e., geometry optimization with inclusion of the bulk solvent effects, indicate a lower energy of **2__2A** compared with **TS2A**. Thus, the single point methodology can be the main reason of the energy discrepancies observed (for more details see the Discussion section, where theoretical vs experimental results concerning the RDS of the reaction are also addressed).

System B. The nucleophilic vinylic substitution of the methoxy group in 3-methoxypropenal by a hydroxide ion is calculated to proceed via a an analogous mechanism as obtained for system A. One major difference concerns the elimination step (**2__2B** → **TS2B** → **3B**) which is in concert with proton transfer (O8−H9 → O1−H9).

Compared with **TS1A**, **TS1B** is formed earlier [*d*(C2−O8) = 0.245 and 0.199 nm, see Figures 1 and 2] and leads to a more stable tetrahedral intermediate **2__1B** (30 − 50 kJ mol^{-1} below the complex **1B**). The resonance delocalization of the charge into the carbonyl group is indicated by the high negative value of the charge on O5 in **2__1B** [-0.51 → −0.65 (O5), −0.09 → −0.20 (C3), **1B** → **2__1B**, B3LYP//B3LYP]. The resonance effect of the electron-withdrawing carbonyl group can also be seen in **TS1B**, which lies less than ≈ 30 kJ mol^{-1} above the complex **1B**. These values of the activation energy are lower by a factor of 2 compared with those of system A. The conversion of **2__1B** to **2__2B** includes rotations of both the C2−C3 and C2−O8 bonds. In the resulting conformation the H9 hydrogen of the hydroxyl group points toward the O1 oxygen (hydrogen bonding between O1 and H9 is indicated by a distance of 0.213 nm). The elimination step (**TS2B**) is in concert with proton transfer (O8−H9 → O1−H9), although it significantly lags behind the breaking of the C2−O1 bond. In contrast to system A, where all methods used indicated the addition step to be rate determining in the gas phase, here somewhat contradictory results are obtained (see Table 2). Additional higher level calculations (MP4//B3LYP, MP2//MP2)[19] indicate that also for system B nucleophilic addition of the hydroxide anion (**1B** → **TS1B** → **2__1B**) will be rate determining. Experimentally, for nucleophilic vinylic substitutions between several anionic nucleophiles (including hydroxide ion) and a variety of vinylic substrates with different activating and leaving groups in 50% Me_2SO−50% H_2O, attack by a hydroxide ion was found to be rate determining.[10b−e] Finally, additional thermodynamic analyses of activation Gibbs free energies ($\Delta G^{\ddagger}$, see Table S2 of the Supporting Information) rather than activation energies ($\Delta E^{\ddagger}$) revealed the same energetic trend for all methods used: $\Delta G_{1B}^{\ddagger}$ is the highest in energy overall. Therefore we conclude that nucleophilic addition of hydroxide ion at the *β*-carbon (**1B** → **TS1B** → **2__1B**) is the RDS of the reaction in agreement with the above-mentioned experimental results.

Inclusion of bulk solvent effects again dramatically increases both barriers. The energy profiles calculated by these methods are at variance with the above-mentioned experimental results.[10b−e] With both methods **TS2B** has the highest energy [$(E_{TS2B})_{rel}$ = 56 and 71 kJ mol^{-1}, respectively]. Therefore, additional calculations with a lager basis set (AUG-cc-pVTZ) were performed. These results (Table 1) provide a more satisfactory energy profile where **TS1B** is now slightly higher (≈ 3 kJ mol^{-1}) than **TS2B**. As was proposed by the kinetics of Bernasconi et al.,[10b−e] addition of hydroxide ion at the *β*-carbon of 3-methoxypropenal (**reactants** → **TS1B** → **2__1B**) also seems to be rate determining in aqueous solution.

System C. Due to the cyclic geometry of 2,3-dihydro-4*H*-pyran-4-one, ring-opening, i.e., elimination, can occur either via outward (**TS2C**) or inward (**TS4C**) rotation of the hydroxy group around the C2−C3 bond of the tetrahedral intermediate (see Scheme 1 and Figure 3). In the latter pathway, additional conformational inter-

(19) Kóňa, J.; Fabian, W. M. F.; Zahradník, P. Unpublished results.

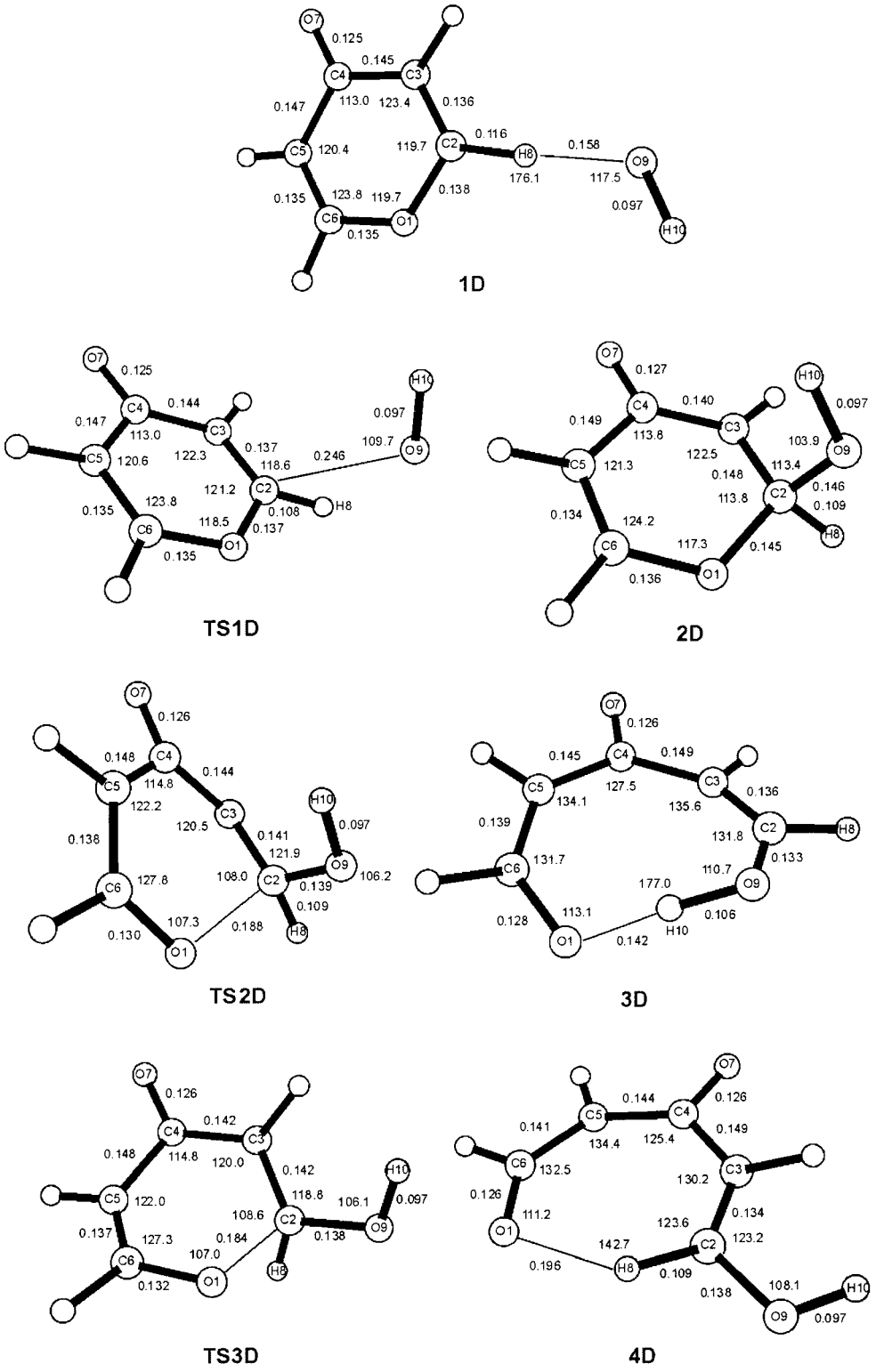

Figure 5. B3LYP calculated structures of the various minima and transition states for nucleophilic vinylic substitution by a hydroxide ion of 4*H*-pyran-4-one. Distances are given in nm and bond angles in degrees.

conversions (**2C** → **TS3C** → **4_1C** → **4_2C**, Scheme 1) are required. Ring opening (**4_2C** → **TS4C** → **5C**) is found to be in concert with proton transfer from the O10 oxygen to the O1 ring oxygen (O10−H11 → O1−H11).

The ring of 2,3-dihydro-4*H*-pyran-4-one is not planar. Hydroxide ion attacks C2 from the side where H9 is axially attached to C6. **TS1C** was found at quite a long O10−C2 distance (see Figure 3). In addition, the complex **1C** is structurally different from the analogous complexes **1A**, **1B**, and **1D**. Hydroxide ion forms a hydrogen bond with the H9 hydrogen attached to the C6 carbon in **1C** (in contrast, in **1A**, **1B**, and **1D**, hydrogen bonds are formed between hydroxide ion and the H8 hydrogen attached to the C2 vinylic carbon, see Figures 1, 2, and 5).

The surprisingly low barrier for addition of the hydroxide ion ($\Delta E_{1B}^{\ddagger} \approx 10$ kJ mol^{-1}) can be explained by the unique geometry of **1C**. The alternative complex

resembling the structures of **1A**, **1B**, and **1D** would lead to an activation energy of 25 kJ mol^{-1}—a value almost identical with $\Delta E_{1B}^{\ddagger}$. Thus, ring strain effects appear to have no significant influence on the addition step (these effects play a crucial role for the ring-opening step, which is discussed below). As in system B, the C4−O7 carbonyl group stabilizes the negatively charged intermediate **2C**. The highest negative value of the charge is again found on O7 in **2C** [−0.54 → −0.68 (O7), 0.09 → −0.23 (C3), **1C** → **2C**, B3LYP//B3LYP]. Both ring-opening processes (Scheme 1) have significantly higher barriers than found in system B (compare $\Delta E_{2C}^{\ddagger}$ and $\Delta E_{4C}^{\ddagger}$ with $\Delta E_{2B}^{\ddagger}$). Therefore, in contrast to both systems A and B, the elimination step is rate determining for the reaction in the gas phase. Let us consider the reverse process, i.e., ring closure (**3C** → **TS2C** → **2C** or **5C** → **TS4C** → **4_2C**). In this case, the nucleophilic oxygen moiety must attack C2 under a very limited range of the valence and torsion angles. The difference between the O1−C2−C3−C4 torsion angle in system B (88.9° in **TS2B**) and system C (43.7° in **TS2C** and 45.1° in **TS4C**) is almost a factor of 2. These structural restrictions are so significant that a change in the reaction mechanism is induced. Furthermore, ring-opening via inward rotation of the hydroxy group, i.e., **1C** → **TS1C** → **2C** → **TS3C** → **4_1C** → **4_2C** → **TS4C** → **5C**, obviously is the preferred mechanism in the gas phase.

In contrast—according to the PCM calculations— in aqueous solution the mechanism **reactants** → **TS1C** → **2C** → **TS2C** → **3C** → **5C**, i.e. ring opening via outward rotation of the hydroxy group, should be more probable. With respect to the rate determining step in aqueous solution, the results depend on the basis set used. At our highest level of theory, addition of the nucleophile should have a slightly higher barrier than ring fission.

System D. Compared to system C, addition of hydroxide ion to C2 has to overcome not only a 3−5 times higher barrier but also leads to a less stable product. This result can be explained by the partial aromatic nature of the γ-pyrone ring. After addition of hydroxide ion, the C2 carbon becomes sp^3 hybridized and the γ-pyrone ring loses its aromatic character. In contrast to system C, both ring-opening processes (via **TS2D** and **TS3D**) can proceed from the same tetrahedral intermediate **2D** as revealed by the IRC calculations starting from either **TS2D** or **TS3D**. Thus, no conformational interconversions are required. It is interesting to note that the hydroxyl group at C2 of this intermediate occupies the axial position. A conformer with an equatorial hydroxyl group does not occur in any of the calculated mechanisms. In contrast to system C, the ring-opening steps take place without any proton transfer. Therefore, intermediates **3D** and **4D** only present a set of *E*/*Z* isomers with respect to the C2−C3 double bond where **3D** is the *Z* and **4D** the *E* isomer. Ring opening proceeding through transition state **TS2D**, i.e., via inward rotation of the hydroxy group (see Scheme 1 and Figure 5), has the highest activation energy but gives the more stable product **3D**. The second mechanism describes ring opening through transition state **TS3D** (outward rotation), which has a somewhat lower activation energy but results in the less stable product **4D**. However, it is well-known that ring-opened products of the reactions of 4*H*-pyran-4-ones and their benzologues with hydroxide ion are unstable and can undergo a variety of transformations, i.e., a conformational interconversion of **4D** to a more stable isomer or sequences of other processes such as recyclization or degradation.[1,5b,8b,c]

As in system C, incorporation of the double bond into a cyclic system changes the mechanism of the reaction in the gas phase in comparison to the acyclic systems A and B. Ring-opening rather than addition of the hydroxide anion is predicted to be rate determining for the isolated molecules. In contrast to system C, γ-pyrone ring opening via outward rotation of the hydroxy group (**TS3D**) should be more feasible. Furthermore, in system D the barrier for the ring-opening step generally is lower than in system C.

In aqueous solution the addition step is endothermic. Compound **2D** lies 24−44 kJ mol^{-1} above the separated reactants. As in the gas phase, ring opening via outward rotation (**TS3D**) is also the preferred pathway in aqueous solution. Concerning the rate-determining step the calculations unambiguously indicate addition of the hydroxide anion rather than elimination (ring opening) as the process with the highest barrier. Therefore, the pathway **reactants** → **TS1D** → **2D** → **TS3D** → **4D** is the most probable mechanism with addition of hydroxide ion at C2 as the RDS in aqueous solution.

The PCM and CosmoPCM calculations with the 6-31+G(d) basis set performed for system D are similar to those calculated on the reaction between 4*H*-1-benzopyran-4-one and hydroxide ion in our previous work.[9] They are in agreement with experimental results of Szabó et al.,[8b,c] where addition of hydroxide ion at C2 of 4*H*-1-benzopyran-4-one was determined to be the RDS of the reaction in aqueous solution.

Discussion

Two quantum-chemical methods, namely Becke's hybrid density functional/HF procedure and second-order Møller−Plesset perturbation theory, were employed to analyze NVS by a hydroxide ion for the four model systems. Except for system B both methods provide similar energetic trends. For gas phase reactions, results obtained by the 6-31+G(d) and AUG-cc-pVTZ basis sets show only little differences. Inclusion of bulk solvent effects via the PCM or CosmoPCM approximations turned out not to be straightforward and the results obtained thereby have to be taken cum grano salis. Specifically, the size of the basis set [6-31+G(d) vs AUG-cc-pVTZ] has a profound influence leading in some cases to a reversal of the predicted RDS. Only for system D the calculations with the medium-sized 6-31+G(d) basis set were able to predict a mechanism in agreement with the experimental results of Szabó et al.[8b,c]

System A turned out to be the most complicated. In this case, the single point calculation methodology for solvent effects indicates some discrepancies, even when the large AUG-cc-pVTZ basis set is used. In other words, changes in energy seem to be very sensitive to changes between the geometries in the gas phase and aqueous solution for system A. On the other hand, as was shown in our previous calculations [9] on NVS between 4*H*-1-benzopyran-4-one and hydroxide ion, the single point calculation methodology can be a good alternative for analyzing larger reaction systems. In this reaction, this methodology provided similar energetic trends as did optimizations with inclusion of bulk solvent effects.

The influence of the activating carbonyl group is mainly transparent for the addition step. Its electron-

withdrawing and resonance effects decrease the activation barrier for the addition step and stabilize the negatively charged tetrahedral intermediates (compare the values for systems A and B in Table 2). On the other hand, the presence of the activating group increases the activation barrier for the elimination step. This can be explained by the concept of "transition state imbalance" formulated by Bernasconi in the Principle of Nonperfect Synchronization.[20] To reach the transition state **TS2B**, i.e., to reach the O1−C2 bond cleavage, the charge has to be localized from the O5 carbonyl oxygen onto the C2 vinylic carbon, which entails loss of the resonance stabilization of the anionic tetrahedral intermediate **2_2B**, a process that requires a large amount of energy. Accordingly, the stronger the resonance stabilization of the anionic tetrahedral intermediate, the larger the intrinsic barrier of the elimination step. In contrast, in system A where the tetrahedral intermediate **2_2A** cannot be stabilized by any resonance delocalization, there is only a small imbalance, and hence the activation barrier is low because not much energy is required to localize the charge from C3 on C2 at **TS2A**.

In addition, our calculations also revealed that the presence of the activating carbonyl group does not change the mechanism of NVS by a hydroxide ion, i.e., as in system A, addition of hydroxide ion at the β-carbon is still the RDS of the reaction in both gas phase and aqueous solution in system B.

An additional increase of the activation energy for the elimination step is observed in the cyclic systems C and D. This is caused by cyclic strain effects, which act in concert with the above-mentioned resonance effects. Consequently, the restrained geometry of the transition state of the ring-opening process is unfavorable for the charge localization and its transfer along the bond which is broken. These effects seem to play a crucial role, because in the calculated cyclic systems the activation barriers for the elimination step are higher than those for the addition step. Thus, a different mechanism of NVS with elimination of the leaving group rather than addition of hydroxide ion as rate determining is indicated in the gas phase. Loss of the aromatic character of the γ-pyrone ring (system D) by addition of the nucleophile greatly increases and decreases the barriers for addition and elimination, respectively. According to the interpretation of Bernasconi,[20] the lower barrier of the elimination step indicates a weaker resonance stabilization by the carbonyl group of the tetrahedral intermediate **2D** as compared with **2B** or **2C**. In other words, aromatic effects act opposite to resonance effects of the activating carbonyl group.

On the basis of the spectroscopic properties,[1,5] 4*H*-pyran-4-one is considered to be more aromatic than its benzologue 4*H*-1-benzopyran-4-one. Consequently, one would expect a lower activation energy of the addition step and higher one of the elimination step for the reaction of 4*H*-1-benzopyran-4-one. This trend was confirmed (see Table 5, values in parentheses) by the calculations.

(20) (a) Bernasconi, C. F. *Acc. Chem. Res.* **1987**, *20*, 301; **1992**, *25*, 9; *Adv. Phys. Org. Chem.* **1992**, *27*, 119. (b) Bernasconi, C. F.; Wenzel, P. J.; Keeffe, J. R.; Gronert, S. *J. Am. Chem. Soc.* **1997**, *119*, 4008. (c) Bernasconi, C. F.; Kittredge, K. W. *J. Org. Chem.* **1998**, *63*, 1944.

Bulk solvent effects dramatically increase the activation parameters for all calculated reactions. In aqueous solution for all systems studied addition of hydroxide ion at the vinylic carbon is rate determining. The energy required for desolvation of the hydroxide ion and an initial charge dispersion in the transition state may be the reason for the high activation energy for the first step. The solvent effects are also responsible for the different mechanism in the gas phase and aqueous solution calculated for the cyclic systems C and D, where inclusion of bulk solvent effects in the calculations changes the RDS of the reaction (elimination of the leaving group as the RDS in the gas phase vs addition of hydroxide ion at C2 as the RDS in aqueous solution).

Conclusions

On the basis of our ab initio and DFT calculations, the basic principles concerning ring-opening reactions of pyranones can be established. Furthermore, some generalizations to nucleophilic substitutions at a vinylic carbon can be made:

(a) In the gas phase the RDS of NVS by a hydroxide ion may be either addition of hydroxide ion at the vinylic carbon or elimination of the leaving group.

(b) In aqueous solution addition of hydroxide ion at the vinylic carbon is the RDS for all systems studied.

(c) The electron-withdrawing carbonyl group decreases the activation energy for the addition step and increases it for the elimination step by resonance stabilization of the tetrahedral intermediate.

(d) Cyclic strain effects mainly affect the ring-opening steps where large increases of the activation energy were observed. They can be the prevailing factor for the determination of the RDS in the gas phase.

(e) Bulk solvent effects are of great significance for NVS of pyranones. Specifically, they can change the mechanism to one where addition of hydroxide ion rather than elimination of the leaving group becomes rate determining.

(f) Aromatic effects increase the activation barrier for the addition step and decrease it for the elimination step.

As we concluded above, ring-opening reactions of 4*H*-pyran-4-ones and their benzologues with anionic oxygen nucleophiles such as hydroxide ion can proceed by different mechanisms depending on strain, resonance, and polar effects. Whereas addition of the nucleophile at C2 is the RDS of the reaction in polar solution, elimination of the leaving group can be expected as rate determining in the gas phase or apolar solution. Finally, it should be stressed that the solvent calculations are by no means straightforward and are, in contrast to the gas phase results, significantly more dependent on the basis set used.

Acknowledgment. The financial support for this research was granted by the Action Austria-Slovakia and ERASMUS/SOCRATES and is gratefully acknowledged.

Supporting Information Available: Tables of total energies including ZPE contributions, total and relative Gibbs free energies, and free energies of solvation. This material is available free of charge via the Internet at http://pubs.acs.org.

JO001222I